

Holographic Krylov Complexity with Lifshitz Scaling and Hyperscaling Violation

Kazem Bitaghsir Fadafan^a and M. Reza Mohammadi Mozaffar^b

^a *Faculty of Physics, Shahrood University of Technology, Shahrood, Iran*

^b *Department of Physics, University of Guilan, P.O. Box 41335-1914, Rasht, Iran*

E-mails: bitaghsir@shahroodut.ac.ir, mmohammadi@guilan.ac.ir

Abstract

Following the holographic proposal that identifies the growth rate of Krylov complexity with the proper radial momentum of an infalling massive probe, we study Krylov complexity in Lifshitz and hyperscaling-violating backgrounds. For pure Lifshitz geometries, we derive exact analytic solutions and obtain quadratic complexity growth for all values of the dynamical exponent. For hyperscaling-violating backgrounds, we extract the asymptotic scaling, revealing that the hyperscaling-violating exponent directly controls the late-time growth exponent. In a special limiting case, the complexity exhibits oscillatory behavior with a logarithmic envelope, signaling a transition to a qualitatively distinct regime. Our analysis establishes that the momentum-Krylov correspondence extends naturally to non-relativistic holographic settings and remains well-defined despite the causal pathologies of Lifshitz spacetimes.

Contents

1	Introduction	1
2	General framework	4
3	Lifshitz background	5
3.1	Geodesic motion of an infalling particle	6
3.2	Generalised proper momentum and complexity	7
4	Hyperscaling-violating generalization	9
4.1	Geodesic motion and complexity	9
4.2	Asymptotic expansions	11
5	Conclusions and discussions	13
A	Detailed derivations for hyperscaling-violating background	15

1 Introduction

The gauge/gravity duality, originating from the AdS/CFT correspondence [1–3], establishes a precise geometric dictionary for strongly coupled quantum field theories, allowing non-perturbative phenomena to be studied using classical gravitational methods in one higher dimension. Within this framework, the holographic computation of quantum information-theoretic quantities has become an active research direction. Measures such as entanglement entropy, mutual information, out-of-time-order correlators (OTOCs), and quantum complexity have been given well-defined gravitational duals [4–10]. These correspondences have provided insights into the emergence of spacetime geometry from entanglement, as well as into black hole interiors, quantum chaos, and thermalization dynamics.

Among these, quantum complexity has received considerable attention in holography. Two prominent proposals have emerged: the complexity-volume (CV) duality, which identifies the complexity of the boundary state with the volume of a maximal codimension-one bulk surface ending on the boundary [8, 9], and the complexity-action (CA) duality, which equates complexity to the gravitational action evaluated on a bulk region known as the Wheeler-DeWitt patch [10]. Both proposals have successfully reproduced expected features of complexity, such as linear growth at late times for black hole backgrounds, and have been extensively studied in various holographic settings. However, they suffer from certain ambiguities, including dependence on the choice of reference state and, in the CV case, on the specific prescription for the codimension-one surface.

A more recent development in the study of quantum many-body dynamics is Krylov complexity, a measure of operator growth [11]. Krylov complexity quantifies the spread of an initially simple

operator under time evolution within an orthonormal Krylov basis, constructed recursively via the Lanczos algorithm. The complexity, defined as the expectation value of the Krylov position operator, serves as a diagnostic of integrability versus chaos, operator scrambling, and thermalization in systems ranging from quantum spin chains and random matrix theory to quantum field theories [12–19]. A precise holographic dual for Krylov complexity has been proposed, linking boundary operator dynamics to bulk geodesic motion [20]. In this proposal, the time derivative of the Krylov complexity $C_K(t)$ in the boundary theory is identified with the proper radial momentum of a massive probe particle moving along a geodesic in the dual bulk geometry

$$\dot{C}_K(t) = -P_\rho, \tag{1.1}$$

where ρ is the proper radial coordinate. This geometric interpretation has been tested in several relativistic holographic backgrounds, including AdS black holes, confining geometries, and the Coulomb branch of $\mathcal{N} = 4$ super Yang-Mills theory [20–25]. These studies have revealed universal features of complexity growth, such as early-time linear or exponential behavior and late-time saturation, often connected to black hole horizons and chaos bounds. The Krylov complexity prescription differs from CV and CA in both concept and scope. CV and CA are holographic conjectures that assign a complexity to the boundary quantum state via bulk geometric quantities. Krylov complexity, by contrast, is a field-theoretic quantity defined from operator growth dynamics, with its holographic dual given by the proper radial momentum of an infalling probe. This provides a state-independent, ambiguity-free geometric dual that is intrinsically dynamical.

Given these advantages, it is natural to ask whether the holographic Krylov complexity prescription applies to non-relativistic bulk backgrounds, whose dual field theories lack Lorentz invariance. This is the central question we address in this work. Specifically, we investigate the scaling and time evolution of Krylov complexity in theories where Lorentz invariance is broken. Such systems are physically well-motivated: many strongly coupled systems in condensed matter physics, including quantum critical points in correlated materials, ultracold atomic gases, and certain non-relativistic gauge theories, exhibit anisotropic scaling symmetries. Their holographic descriptions are provided by Lifshitz geometries, often with hyperscaling violation [26–28], which are invariant under the generalized scaling transformation

$$t \rightarrow \lambda^z t, \quad x^i \rightarrow \lambda x^i, \quad r \rightarrow \lambda^{-1} r, \quad ds \rightarrow \lambda^{\theta/d} ds, \tag{1.2}$$

where z is the dynamical critical exponent, θ is the hyperscaling-violating exponent, and d is the spatial dimension. The effective dimensionality of the system is given by $d_{\text{eff}} = d - \theta$. These geometries arise naturally in Einstein-dilaton-Maxwell theories and string theory embeddings, providing a controlled setting for non-relativistic holography [29].

Extending the holographic formulation of Krylov complexity to these non-relativistic backgrounds is timely. The dynamical exponent z controls the relative scaling of time and space, affecting dispersion relations, transport, and information scrambling. The hyperscaling-violating

exponent θ introduces additional scaling dimensions that can alter critical behavior. Understanding how these parameters influence operator growth may reveal new universal features of quantum chaos and complexity in anisotropic systems and possibly lead to generalized bounds on complexity growth rates beyond the relativistic regime [30]. In this direction, quantum chaos, entanglement measures, and computational complexity in Lifshitz theories have been extensively studied in recent years on the field theory side, leading to a rich variety of new results [31–44].

Holographic Krylov (spread) complexity has been extensively tested across a variety of backgrounds [22–25, 45]. In confining holographic geometries with a smooth infrared end-of-space, a robust and universal feature emerges: Krylov complexity exhibits oscillatory behaviour, with frequency controlled by the confinement scale. These oscillations have been shown to qualitatively match field-theoretic results from the longitudinally perturbed Ising model, suggesting they constitute a universal signature of confinement and a sensitive probe of infrared reorganisation in strongly coupled quantum field theories [22, 23]. Recent studies have extended this framework to higher-dimensional superconformal field theories and top-down Type IIB solutions describing twisted-circle compactifications of $\mathcal{N} = 4$ SYM [24, 25, 45]. For example, in strongly coupled six-dimensional superconformal field theories with holographic duals in massive Type IIA supergravity [45], the dynamics of massive geodesic probes have been analysed, allowing the bulk particle to move along radial and internal directions. In the dual field theory, these motions encode operator growth and the associated global symmetries.

In this work, we systematically develop the holographic computation of Krylov complexity in geometries with Lifshitz scaling and hyperscaling violation. It is worth noting that Lifshitz and Schrödinger solutions in higher-dimensional supergravity typically do not accommodate simple geodesic motion along internal directions. We have verified, for instance, that in the supergravity solutions of Ref. [46], extending the analysis to include motion along the internal space is not straightforward in the context of purely radial motion. We therefore restrict our attention to geometries with Lifshitz scaling and hyperscaling violation, where we consider massive probe particles and derive the conserved quantities associated with the Killing symmetries of the background. Solving the geodesic equations, we obtain explicit expressions for the canonical and proper radial momenta, from which we compute the time dependence of $\dot{C}_K(t)$ and analyze its dependence on z , θ , and the probe mass m .

The paper is organized as follows. In Section 2, we review the holographic proposal for Krylov complexity and establish the general framework for computing proper radial momentum in arbitrary bulk backgrounds. We then introduce the Lifshitz and hyperscaling-violating geometries that will be the focus of our analysis, and discuss the constraints imposed by the null energy condition. Section 3 is devoted to pure Lifshitz backgrounds: we derive the geodesic equations for a massive infalling probe, compute the canonical and proper radial momenta, and obtain the time evolution of Krylov complexity. We also discuss the pathologies of Lifshitz spacetimes and explain why they do not affect our calculation. Section 4 generalizes the analysis to hyperscaling-violating geometries, where we derive the trajectory and momenta in terms of hypergeometric functions,

and provide systematic early-time and late-time asymptotic expansions. Section 5 summarizes our main findings and outlines promising future directions, including extensions to probes with internal structure and connections to other quantum information measures in non-relativistic holography. We relegate some details of the computations to the appendix.

2 General framework

In the following sections, we apply the holographic prescription of [20] to determine the time evolution of Krylov complexity in the boundary theory using Eq. (1.1). To establish the general framework, consider a bulk background with a metric of the form

$$ds^2 = G_{00}(r)dt^2 + G_{rr}(r)dr^2 + G_{ij}(r)dx^i dx^j + (\text{internal space}), \quad (2.1)$$

where r is the radial holographic coordinate, with the conformal boundary located at $r \rightarrow 0$. We assume the metric components depend only on r , reflecting translational invariance in the boundary spatial directions x^i and time t . We discuss the effect of the internal space at the end of this section.

To compute Krylov complexity, we introduce a proper distance coordinate ρ along the radial direction. The proper radial distance is defined by

$$d\rho^2 = G_{rr}(r)dr^2. \quad (2.2)$$

This coordinate change is essential because the holographic proposal identifies the growth rate of Krylov complexity with the proper radial momentum rather than the coordinate momentum [20]. We consider an infalling probe — which may be a particle, string, or brane — moving along a radial geodesic [25]. The probe is subject to the initial conditions

$$r(0) = \epsilon, \quad \dot{r}(0) = 0, \quad (2.3)$$

where ϵ is a UV cutoff near the boundary. These conditions correspond to releasing the probe from rest at the UV boundary at time $t = 0$. The probe then falls inward under the influence of the bulk gravitational field.

Let \mathcal{L} denote the Lagrangian of the probe. The canonical momentum conjugate to the proper radial coordinate ρ is given by

$$P_\rho = \frac{\partial \mathcal{L}}{\partial \dot{\rho}}, \quad (2.4)$$

where the dot denotes differentiation with respect to the affine parameter (typically proper time). This momentum is conserved if the background possesses appropriate Killing symmetries; in particular, time translation invariance yields conservation of the energy $E = -\partial \mathcal{L} / \partial \dot{t}$.

According to the holographic proposal for Krylov complexity, the rate of change of Krylov complexity in the boundary theory is identified with the proper radial momentum of the infalling

probe [20]

$$\dot{C}_K(t) = -P_\rho(t). \quad (2.5)$$

The negative sign ensures that complexity grows as the probe falls inward (since P_ρ is negative for infalling motion). Thus, by solving the geodesic equations for the probe and computing P_ρ as a function of boundary time t , we obtain the time evolution of Krylov complexity in the dual field theory.

We now specialize to backgrounds with a general dynamical critical exponent z and hyperscaling violation exponent θ . These theories admit a fixed point invariant under the anisotropic scaling transformation in Eq. (1.2). A number of holographic aspects of these theories have been studied in [47–52]. Consider a $(d + 2)$ -dimensional solution in Einstein gravity coupled to appropriate matter fields (see, e.g., [47])

$$ds^2 = \frac{1}{r^{2(d-\theta)/d}} \left(-\frac{1}{r^{2(z-1)}} dt^2 + dr^2 + d\vec{x}^2 \right). \quad (2.6)$$

As noted in [47], the null energy condition imposes the bounds

$$(d - \theta)(d(z - 1) - \theta) \geq 0, \quad (z - 1)(d - \theta + z) \geq 0, \quad (2.7)$$

also, entanglement entropy analysis and string theory realizations of hyperscaling-violating geometries suggest inconsistency when $\theta > d$.

Note that the metric in Eq. (2.1) generically includes an internal space. The role of such internal spaces in holographic Krylov complexity was investigated in Ref. [25] for a massive particle in $\text{AdS}_5 \times S^5$ carrying conserved R-charge. It was shown that motion in the internal space modifies complexity growth, providing a holographic realization of symmetry-resolved Krylov complexity. Since our background in Eq. (2.6) does not include an internal space, we do not consider such effects in this work.

Now equipped with all the necessary tools, we proceed to calculate the time evolution of Krylov complexity. Unfortunately, it is not possible to obtain an analytic expression for the growth rate in a general setup. In the following, we present numerical results along with analytic treatments for specific cases.

3 Lifshitz background

We now specialize to a Lifshitz geometry with a nontrivial dynamical exponent z , and study Krylov complexity using the holographic prescription outlined above. We first analyze the geodesic motion of an infalling massive particle, and then compute the associated proper momentum, from which the complexity growth rate follows via Eq. (2.5).

3.1 Geodesic motion of an infalling particle

We consider a massive particle moving in a Lifshitz spacetime, which is dual to a boundary state with nonrelativistic scaling symmetry. The metric is obtained by setting $\theta = 0$ in Eq. (2.6)

$$ds^2 = -\frac{dt^2}{r^{2z}} + \frac{dr^2 + d\vec{x}^2}{r^2}. \quad (3.1)$$

For radial geodesics, we set $d\vec{x} = 0$. Defining the proper time interval as $d\tau^2 = -ds^2$ and using the above equation, we obtain

$$d\tau = \frac{dt}{r^z} \sqrt{1 - r^{2z-2}\dot{r}^2}, \quad (3.2)$$

where the dot denotes differentiation with respect to t . Note that the proper time is real only when the expression under the square root is non-negative, i.e., $r^{2z-2}\dot{r}^2 \leq 1$, which imposes a constraint on the allowed radial velocities. In the relativistic limit $z = 1$, this condition reduces to the familiar bound $\dot{r}^2 \leq 1$. Using the relation above, the action for a massive particle of mass m takes the form

$$S = -m \int \frac{dt}{r^z} \sqrt{1 - r^{2z-2}\dot{r}^2} \equiv \int \mathcal{L}(r, \dot{r}) dt. \quad (3.3)$$

Since the Lagrangian has no explicit time dependence, the corresponding Hamiltonian (energy) is conserved

$$H = \dot{r} \frac{\partial \mathcal{L}}{\partial \dot{r}} - \mathcal{L} = \text{constant}. \quad (3.4)$$

Denoting this constant energy by E , a straightforward calculation yields

$$E = \frac{m}{r^z \sqrt{1 - r^{2z-2}\dot{r}^2}} = \frac{m}{\epsilon^z}, \quad (3.5)$$

where in the second equality we have used the initial conditions in Eq. (2.3) to express the energy in terms of the UV cutoff ϵ . Solving Eq. (3.5) for \dot{r}^2 , we obtain the radial velocity squared

$$\dot{r}^2 = r^{2-2z} \left(1 - \left(\frac{\epsilon}{r} \right)^{2z} \right). \quad (3.6)$$

We always choose the positive square root, corresponding to the particle falling inward from the UV boundary ($\dot{r} > 0$ for $t > 0$). For the relativistic case $z = 1$, this reduces to the familiar AdS result $\dot{r}^2 = 1 - (\epsilon/r)^2$. For $z > 1$, the velocity is suppressed at small r by the factor r^{2-2z} , indicating that the particle takes longer to approach the deep interior. Now, solving the differential equation for $r(t)$ with the initial condition $r(0) = \epsilon$, we obtain

$$r(t) = (\epsilon^{2z} + z^2 t^2)^{\frac{1}{2z}}. \quad (3.7)$$

Again, for $z > 1$, the growth of $r(t)$ is slower at early times due to the exponent $1/(2z)$.

These results reveal several key features of the geodesic motion in the Lifshitz background. For $z = 1$, which corresponds to the AdS case, the radial coordinate grows linearly at late times,

$r(t) \sim t$, and the velocity approaches a constant, $\dot{r}(t) \rightarrow 1$. For $z > 1$, the late-time behavior of the radial coordinate is given by $r(t) \sim t^{1/z}$, which implies that the velocity scales as $\dot{r}(t) \sim t^{1/z-1}$. Since $1/z - 1 < 0$ for $z > 1$, the velocity decays as a power law at late times, reflecting the slower infall of the particle into the interior compared to the relativistic case. The decay exponent becomes more negative as z increases, indicating that larger values of the dynamical exponent lead to a more significant suppression of the radial velocity. The regime $z < 1$ is forbidden by the null energy condition and is therefore not considered. These features are summarized in Figure 1.

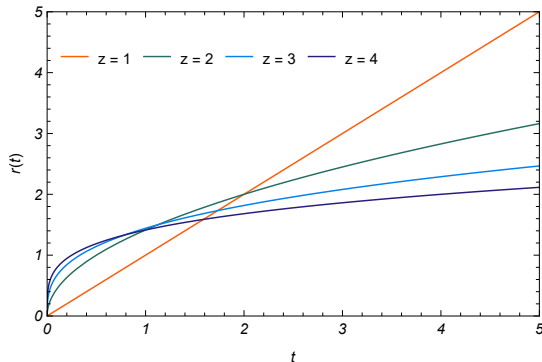


Figure 1: The trajectory $r(t)$ of the infalling particle in the Lifshitz geometry for several values of the dynamical exponent z , with $\epsilon = 0.01$. For larger z , the particle takes longer to reach a given radial coordinate. The slope of the curves indicates power-law decay of the velocity for $z > 1$, in contrast to the constant asymptotic velocity observed for $z = 1$.

Before proceeding to the computation of Krylov complexity, it is important to address potential concerns regarding the applicability of the holographic prescription in Lifshitz backgrounds. Lifshitz spacetimes exhibit several pathologies that distinguish them from the well-behaved AdS case, including null curvature singularities, trapping of non-radial null geodesics, degeneracy of causal wedges, and, in certain string theory embeddings, closed timelike curves [27, 53–55]. These features indicate that the standard holographic dictionary requires substantial revision for non-relativistic geometries. However, the specific nature of our calculation circumvents these obstructions. We consider only purely radial motion with no transverse momentum, which avoids the trapping of geodesics and the associated causal wedge degeneracy. The proper momentum prescription for Krylov complexity depends only on the local geometry along the radial geodesic and remains well-defined regardless of global causal pathologies. Thus, while the reconstruction of general bulk surfaces from boundary data may be obstructed in Lifshitz backgrounds, the momentum-Krylov correspondence remains applicable for the radial probes considered in this work.

3.2 Generalised proper momentum and complexity

Having established the trajectory and geodesic motion of a massive particle in the Lifshitz background, we now study the scaling and evolution of Krylov complexity using the prescription in Eq. (1.1). To this end, we first compute two relevant radial momenta: the canonical momentum

P_r conjugate to the original radial coordinate r , and the proper momentum P_ρ conjugate to the proper radial distance ρ . Recall that the latter is directly identified with the growth rate of Krylov complexity.

Using the Lagrangian defined in Eq. (3.3), the radial momentum conjugate to r is given by

$$P_r = \frac{\partial \mathcal{L}}{\partial \dot{r}} = \frac{m r^{z-2} \dot{r}}{\sqrt{1 - r^{2z-2} \dot{r}^2}}. \quad (3.8)$$

Substituting the velocity $\dot{r}(t)$ from Eq. (3.6) into the above expression, we obtain

$$P_r = \frac{m}{r} \sqrt{\left(\frac{r}{\epsilon}\right)^{2z} - 1}. \quad (3.9)$$

Having obtained P_r , we now examine its behavior in different regimes. Near the boundary, where $r \rightarrow \epsilon$ (early times), the square root vanishes, so $P_r \rightarrow 0$. This is consistent with the initial condition that the probe is released from rest at the UV cutoff. In the deep interior, $r \rightarrow \infty$ (late times), the square root tends to 1, and the prefactor scales as r^{z-1} . For $z = 1$, P_r approaches the constant $m\epsilon^{-1}$. For $z > 1$, P_r grows without bound as r^{z-1} , reflecting the increasing canonical momentum as the particle falls inward.

With the canonical momentum at hand, we now turn to the proper momentum P_ρ , which enters directly in the holographic prescription for Krylov complexity. Based on Eq. (2.2) The proper radial coordinate ρ is defined by $d\rho = r^{-1}dr$, which ensures that the radial part of the metric becomes $d\rho^2$ in the new coordinate. The proper momentum is then

$$P_\rho = \frac{\partial \mathcal{L}}{\partial \dot{\rho}} = r P_r, \quad (3.10)$$

where we have used $\frac{\partial r}{\partial \rho} = r$. Substituting Eq. (3.9) into the above expression, we obtain the explicit form of the proper momentum

$$P_\rho = m \sqrt{\left(\frac{r}{\epsilon}\right)^{2z} - 1}. \quad (3.11)$$

To find the time dependence of this quantity, we employ the geodesic solution $r(t)$ from Eq. (3.7). Inserting this into Eq. (3.11) and simplifying the corresponding expressions, we arrive at

$$P_\rho(t) = \frac{mz}{\epsilon^z} t. \quad (3.12)$$

Note that we have chosen the positive sign since the proper momentum increases with time as the particle falls inward. This result reduces to the known expression in the relativistic limit $z = 1$ reported in [20].

Having obtained the proper momentum, the Krylov complexity follows directly from the holographic prescription in Eq. (2.5). Integrating $\dot{C}_K(t) = -P_\rho(t)$ with the initial condition $C_K(0) = 0$

gives

$$C_K(t) = \int_0^t P_\rho(t') dt' = \frac{mz}{2\epsilon^z} t^2. \quad (3.13)$$

Thus, for all values of the dynamical exponent z , Krylov complexity exhibits universal quadratic growth at zero temperature, with the z -dependence appearing only in the overall coefficient.

The growth rate $\dot{C}_K(t) \sim P_\rho(t)$ is linear in time, with a coefficient proportional to z , while the exponent of t is independent of the dynamical exponent. Consequently, Krylov complexity scales quadratically, $C_K(t) \sim t^2$, for all z . Thus, the non-relativistic scaling symmetry does not constrain the functional form of complexity growth; its only effect is an overall z -dependent factor in the rate.

4 Hyperscaling-violating generalization

We now generalize the previous analysis to include the hyperscaling-violating exponent θ . As we will see, the presence of θ introduces new scaling dimensions that modify both the geodesic motion and the growth of Krylov complexity. We begin by deriving the particle trajectory in the hyperscaling-violating background and computing the associated proper momentum. For generic values of the parameters, the time evolution of the proper momentum and complexity cannot be expressed in closed analytic form; however, the asymptotic behavior can be extracted systematically, which we present in the following subsections.

4.1 Geodesic motion and complexity

The metric in Poincaré-like coordinates is given by Eq. (2.6). We consider a radial geodesic with $\vec{x} = \text{constant}$, which we set to zero by translation invariance. The particle is initially released from rest at $r(0) = \epsilon$, so that $\dot{r}(0) = 0$. For a trajectory with $d\vec{x} = 0$, the metric reduces to

$$ds^2 = -r^{-2z+2\theta/d} dt^2 + r^{-2+2\theta/d} dr^2. \quad (4.1)$$

Using the proper time interval $d\tau^2 = -ds^2$, the action for a massive particle of mass m takes the form

$$S = -m \int r^{-z+\theta/d} \sqrt{1 - r^{2z-2} \dot{r}^2} dt. \quad (4.2)$$

Since the Lagrangian $\mathcal{L}(r, \dot{r})$ has no explicit time dependence, the associated Hamiltonian (energy) is conserved. Denoting this constant by E , a straightforward calculation yields

$$E = \frac{m r^{-z+\theta/d}}{\sqrt{1 - r^{2z-2} \dot{r}^2}} = m \epsilon^{-z+\theta/d}, \quad (4.3)$$

where the second equality follows from evaluating the expression at the initial position $r = \epsilon$ with $\dot{r} = 0$. Solving Eq. (4.3) for the radial velocity squared gives

$$\dot{r}^2 = r^{2-2z} \left(1 - \left(\frac{\epsilon}{r} \right)^{2z-2\theta/d} \right). \quad (4.4)$$

In what follows, we choose the positive square root, corresponding to the particle falling inward from the UV boundary ($\dot{r} > 0$ for $t > 0$). Integrating the above equation and employing the initial conditions, we find

$$t = \frac{r^z}{z} {}_2F_1 \left(\frac{1}{2}, \frac{dz}{2\theta - 2dz}; 1 + \frac{dz}{2\theta - 2dz}; \left(\frac{r}{\epsilon} \right)^{\frac{2\theta}{d} - 2z} \right) + \epsilon^z \frac{d\sqrt{\pi} \Gamma \left(\frac{dz}{2\theta - 2dz} \right)}{(\theta - 2dz) \Gamma \left(-1 + \frac{\theta}{2\theta - 2dz} \right)}, \quad (4.5)$$

where ${}_2F_1$ is the hypergeometric function. In general, it is not possible to find an explicit closed-form expression for $r(t)$, and a numerical illustration is required.

Let us now compute the two relevant radial momenta: the canonical momentum P_r conjugate to the coordinate r , and the proper momentum P_ρ conjugate to the proper radial distance ρ . The canonical momentum is given by

$$P_r = \frac{\partial \mathcal{L}}{\partial \dot{r}} = \frac{m r^{z+\theta/d-2} \dot{r}}{\sqrt{1 - r^{2z-2} \dot{r}^2}}. \quad (4.6)$$

Substituting the velocity expression from Eq. (4.4) into the above equation, we obtain

$$P_r = m \epsilon^{-z+\theta/d} r^{z-1} \sqrt{1 - \left(\frac{\epsilon}{r} \right)^{2z-2\theta/d}}. \quad (4.7)$$

With the expression for P_r at hand, we now explore its behavior across different regimes. Near the boundary the square root vanishes and hence $P_r \rightarrow 0$, which is consistent with the probe starting from rest at the UV cutoff. In the opposite limit, deep in the interior, the square root approaches unity and the prefactor scales as r^{z-1} . Interestingly, this power-law growth is independent of θ , implying that the late-time divergence of P_r is dictated solely by the dynamical exponent z . The hyperscaling-violating exponent θ only enters through the normalization factor $\epsilon^{-z+\theta/d}$. For $z = 1$, P_r tends to a finite constant $m\epsilon^{-1+\theta/d}$, which differs from the standard AdS result due to the presence of θ . For $z > 1$, P_r diverges as r^{z-1} , reflecting the steady growth of canonical momentum as the particle falls deeper into the bulk. In contrast to the Lifshitz case, where the normalization was ϵ^{-z} , here the presence of θ modifies the effective UV scale without altering the IR scaling behavior.

The proper radial coordinate ρ is defined by $d\rho = r^{\theta/d-1} dr$, which ensures that the radial part of the metric becomes $d\rho^2$ in the new coordinate. The proper momentum is then given by

$P_\rho = m d\rho/d\tau$, and a straightforward computation yields

$$P_\rho = m \epsilon^{-z+\theta/d} r^{z-\theta/d} \sqrt{1 - \left(\frac{\epsilon}{r}\right)^{2z-2\theta/d}}. \quad (4.8)$$

Note that the two momenta are related by $P_\rho = r^{1-\theta/d} P_r$. For $\theta = 0$, this relation reduces to the Lifshitz result $P_\rho = r P_r$, as expected. In general, it is not possible to find the time dependence of complexity analytically, but an asymptotic expansion is possible, as we carry out in the next section.

4.2 Asymptotic expansions

In this section, we determine the early-time and late-time scaling of Krylov complexity for generic values of the Lifshitz and hyperscaling-violating exponents. Using Eq. (4.5), we analyze the behavior of the geodesic solution in the relevant limits.¹

At early times, corresponding to $r \rightarrow \epsilon$, we obtain the expansion

$$t = \frac{\sqrt{2} \epsilon^{z-1/2} \sqrt{r-\epsilon}}{\sqrt{z-\theta/d}} \left(1 + \frac{3d(2z-1) - 2\theta}{12d\epsilon} (r-\epsilon) \right) + \dots. \quad (4.9)$$

Inverting this relation to express r in terms of t , we find

$$r = \epsilon \left(1 + \frac{dz-\theta}{2d} \left(\frac{t}{\epsilon^z}\right)^2 + \frac{(2\theta + 3d(1-2z))(dz-\theta)^2}{24d^3} \left(\frac{t}{\epsilon^z}\right)^4 \right) + \dots. \quad (4.10)$$

These expansions capture the leading corrections to the initial position as the particle begins to fall inward. For $\theta = 0$, they reduce to the Lifshitz results derived in the previous section, with the first correction scaling as t^2 and a coefficient that depends on both z and θ .

Using the expression for the canonical momentum in Eq. (4.7), together with the early-time expansion for $r(t)$, we obtain

$$P_r = \frac{m(dz-\theta)}{d\epsilon^{1-\theta/d}} \frac{t}{\epsilon^z} \left(1 - \frac{(3d-2\theta)(dz-\theta)}{6d^2} \left(\frac{t}{\epsilon^z}\right)^2 \right) + \dots. \quad (4.11)$$

Similarly, the proper momentum P_ρ from Eq. (4.8) gives

$$P_\rho = \frac{m(dz-\theta)}{d} \frac{t}{\epsilon^z} \left(1 - \frac{\theta(dz-\theta)}{6d^2} \left(\frac{t}{\epsilon^z}\right)^2 \right) + \dots. \quad (4.12)$$

These expressions reveal that both momenta grow linearly in time at leading order, with coefficients proportional to $(dz-\theta)/d$, which vanishes when $\theta = dz$, signaling a special limiting case. In the

¹For completeness, we also provide the detailed algebraic steps underlying the asymptotic expansions in Appendix A.

relativistic limit ($z = 1, \theta = 0$), the above expansions reduce to the familiar results

$$P_r = \frac{mt}{\epsilon^2} - \frac{mt^3}{2\epsilon^4} + \dots, \quad P_\rho = \frac{mt}{\epsilon} + \dots. \quad (4.13)$$

Thus, at early times, the hyperscaling-violating exponent modifies the amplitude of the linear growth while preserving its functional form.

We now turn to the late-time behavior, which exhibits distinct scaling regimes depending on the value of θ relative to dz . Starting from Eq. (4.5), at late times $r \rightarrow \infty$ (assuming $\frac{2\theta}{d} - z < 0$ for convergence of the hypergeometric series), we obtain

$$r = (zt)^{1/z} \left(1 + \frac{d}{2(dz - 2\theta)} \left(\frac{zt}{\epsilon^z} \right)^{\frac{2\theta}{dz} - 2} \right) + \dots. \quad (4.14)$$

This asymptotic form captures the leading power-law growth of the radial coordinate, with sub-leading corrections controlled by the combination $dz - 2\theta$. For $\theta = 0$, this reduces to the Lifshitz result $r \sim (zt)^{1/z}$. Substituting the above expansion into the expressions for the canonical and proper momenta, we find the late-time scaling

$$P_r = m \epsilon^{\theta/d-z} (zt)^{1-1/z}, \quad (4.15)$$

$$P_\rho = m \epsilon^{\theta/d-z} (zt)^{1-\theta/(dz)}. \quad (4.16)$$

These results reveal several important features. First, the canonical momentum P_r scales as $t^{1-1/z}$, which is independent of θ and matches the Lifshitz result. In contrast, the proper momentum P_ρ exhibits a modified exponent $1 - \theta/(dz)$, which explicitly depends on the hyperscaling-violating exponent. For $\theta > 0$, the growth of P_ρ is suppressed compared to the Lifshitz case, while for $\theta < 0$, it is enhanced. In the relativistic limit ($z = 1, \theta = 0$), the above expressions reduce to

$$P_r = \frac{m}{\epsilon} + \dots, \quad P_\rho = \frac{mt}{\epsilon} + \dots. \quad (4.17)$$

Thus, the relativistic limit recovers the expected constant canonical momentum and linearly growing proper momentum, in agreement with known results in the literature.

The corresponding complexity growth follows from integration. At early times, Eq. (4.12) yields

$$C_K(t) = \frac{m(dz - \theta)}{2d} \frac{t^2}{\epsilon^z} + \mathcal{O}(t^4), \quad (4.18)$$

while the late-time scaling from Eq. (4.16) gives

$$C_K(t) \sim \frac{m \epsilon^{\theta/d-z}}{2z - \theta/d} (zt)^{2-\theta/(dz)}. \quad (4.19)$$

This explicitly shows that the hyperscaling-violating exponent modifies the power law of complexity growth at late times.

The expansion in Eq. (4.19) breaks down when $\theta = 2dz$, as the prefactor $2 - \theta/(dz)$ vanishes. In this special case, a separate treatment is required. The action simplifies considerably, and the resulting Lagrangian leads to a conserved energy $E = m\epsilon^z$. The radial velocity squared then takes the form

$$\dot{r}^2 = r^{2-2z} \left(1 - \left(\frac{r}{\epsilon} \right)^{2z} \right). \quad (4.20)$$

Integrating this equation and imposing the initial condition $r(0) = \epsilon$, we find

$$r(t) = \epsilon \left(\cos \frac{zt}{\epsilon^z} \right)^{1/z}. \quad (4.21)$$

In this case, the proper momentum is given by

$$P_\rho = -m \tan \frac{zt}{\epsilon^z}, \quad (4.22)$$

which yields a Krylov complexity of the form

$$C_K(t) \sim \frac{m\epsilon^z}{z} \log \left(\cos \frac{zt}{\epsilon^z} \right). \quad (4.23)$$

This expression exhibits a logarithmic dependence on the cosine, giving rise to oscillatory behavior. Consequently, the complexity is not simply logarithmic in time, but rather oscillatory with a logarithmic envelope. The above result reduces to the early-time expression in Eq. (4.18) and displays oscillatory behavior at late times, with periodic divergences at $t = (\pi/2)(\epsilon^z/z)$. This suggests that the present case is qualitatively distinct from the generic hyperscaling-violating regime and may indicate a transition to a different phase of complexity growth. It is worth noting that the null energy condition imposes nontrivial constraints on the allowed parameter space. For the special case $\theta = 2dz$, the NEC requires $\frac{d}{2d-1} \leq z \leq 1$. Hence, the logarithmic and oscillatory behavior described above is realized only within this restricted range of the dynamical exponent.

Moreover, for the special case $\theta = d$ with $z = 1$, the action simplifies considerably and the conserved energy becomes $E = m$. The radial velocity squared then vanishes identically, and after imposing the initial condition we find that the particle remains at a fixed radial position. Consequently, the proper momentum is identically zero, which implies that the Krylov complexity growth rate vanishes, $\dot{C}_K(t) = 0$, and the complexity remains constant at all times. This case corresponds to a trivial geodesic where the probe does not fall inward, and thus no complexity growth occurs.

5 Conclusions and discussions

In this work, we have systematically investigated the holographic Krylov complexity in non-relativistic backgrounds characterized by Lifshitz scaling and hyperscaling violation. Following the proposal that the time derivative of Krylov complexity is identified with the proper radial

momentum of an infalling massive probe, we have analyzed radial geodesic motion in both pure Lifshitz and hyperscaling-violating geometries.

For the pure Lifshitz case, we derived exact analytic expressions for the radial trajectory, the canonical momentum, and the proper momentum. The geodesic solution takes the simple form $r(t) = (\epsilon^{2z} + z^2 t^2)^{1/(2z)}$, which yields a proper momentum growing linearly in time, $P_\rho(t) = (mz/\epsilon^z)t$. Consequently, Krylov complexity scales quadratically, $C_K(t) \sim t^2$, for all values of the dynamical exponent z . Thus, the non-relativistic scaling symmetry does not constrain the functional form of complexity growth; its only effect is an overall z -dependent factor in the rate.

For the hyperscaling-violating generalization, the presence of θ introduces new scaling dimensions that modify both the geodesic motion and the complexity growth. While an explicit closed-form solution for $r(t)$ is not available for generic parameters, we derived exact expressions for the radial velocity and momenta in terms of hypergeometric functions, and extracted the asymptotic behavior analytically. At late times, the proper momentum scales as $P_\rho \sim t^{1-\theta/(dz)}$, revealing that the hyperscaling-violating exponent controls the growth exponent directly. For $\theta = 0$, the Lifshitz result is recovered, while for $\theta = dz$, the proper momentum approaches a constant, corresponding to logarithmic complexity growth. The relativistic AdS limit ($z = 1, \theta = 0$) reproduces the known result $P_\rho \sim t$.

Beyond the specific results, our work provides a concrete realization of the holographic Krylov complexity dictionary in non-relativistic settings. It demonstrates that the momentum-Krylov correspondence extends beyond conformal backgrounds and remains applicable even in geometries with causal pathologies, provided one restricts to purely radial probes. This is particularly relevant given that Lifshitz spacetimes exhibit null curvature singularities, trapping of non-radial null geodesics, and causal wedge degeneracies that complicate holographic reconstruction. Our analysis shows that the proper momentum prescription, being local along the radial geodesic, circumvents these obstructions. It is instructive to compare our results with the CV and CA holographic complexity proposals in the same backgrounds. For the zero-temperature Lifshitz geometry, both CV and CA complexity exhibit quadratic growth in time, with the dynamical exponent z entering only in the overall coefficient [52]. This matches our finding for Krylov complexity, suggesting that quadratic growth is a universal feature of quantum complexity in non-thermal states, independent of the specific holographic prescription. For hyperscaling-violating backgrounds, the late-time behavior of CV and CA complexity also shows θ -dependent modifications [52], analogous to our result $C_K \sim t^{2-\theta/(dz)}$. However, unlike CV and CA, the Krylov complexity prescription is intrinsically state-independent and free from ambiguities associated with reference states or boundary terms [20], making it a more direct probe of operator growth dynamics in the dual field theory.

As mentioned earlier, Krylov complexity has also been studied directly in non-relativistic quantum field theories. In Refs. [42, 43], various aspects of this measure were analyzed for free bosonic and fermionic field theories with Lifshitz scaling symmetry. In particular, the authors found that for a continuum massless Lifshitz scalar theory, Krylov complexity exhibits exponential growth in time, with the growth rate decreasing as the dynamical exponent z is increased. Interestingly, the

late-time slope remains independent of z . Similar behavior was observed in the fermionic case. It is worth noting that these field-theoretic results were obtained at finite temperature, a regime where the holographic prescription appears to break down or require significant modification. This highlights the complementary nature of the two approaches: holographic computations at zero temperature yield power-law or logarithmic growth, while direct field-theory analyses at finite temperature exhibit exponential behavior. A complete understanding of Krylov complexity in Lifshitz theories would likely require bridging these two regimes.

There are several promising directions for future research. First, incorporating probes with internal structure or extended operators would provide a richer understanding of how non-relativistic symmetries affect symmetry-resolved and operator-dependent complexity. Second, investigating the connection between Krylov complexity and other quantum information measures, such as entanglement entropy or circuit complexity, in Lifshitz holography would help establish a more complete picture of information dynamics in non-relativistic quantum field theories. Finally, it would be interesting to explore whether the oscillatory behavior of Krylov complexity, recently identified as a universal signature of confinement, also appears in certain classes of Lifshitz or hyperscaling-violating geometries with an IR end-of-space.

Overall, our results establish a systematic framework for computing holographic Krylov complexity in non-relativistic backgrounds and highlight the rich interplay between scaling symmetries, geodesic motion, and operator growth.

Acknowledgements

We are very grateful to Carlos Nunez for correspondence, careful reading of the manuscript and his valuable comments.

A Detailed derivations for hyperscaling-violating background

In this appendix, we provide the detailed algebraic steps underlying the asymptotic expansions presented in Section 4. For clarity, we work with the hyperscaling-violating metric in Eq. (2.6) and use the notation $a \equiv z - \theta/d$ for the early-time analysis. For early times, the probe remains near the UV cutoff, so $r \rightarrow \epsilon$. Defining the small parameter $\delta \equiv r - \epsilon$, we start from the velocity squared in Eq. (4.4),

$$\dot{r}^2 = r^{2-2z} \left[1 - \left(\frac{\epsilon}{r} \right)^{2z-2\theta/d} \right]. \quad (\text{A.1})$$

Expanding near $r = \epsilon$ gives $\dot{r} \approx \epsilon^{1/2-z} \sqrt{2a} \sqrt{\delta}$, where we take the positive root for infalling motion. The time integral becomes

$$t = \int_0^\delta \frac{d\delta'}{\dot{r}} = \frac{\sqrt{2} \epsilon^{z-1/2}}{\sqrt{a}} \sqrt{\delta}, \quad (\text{A.2})$$

which, upon inversion, yields the early-time radial trajectory

$$r(t) = \epsilon \left(1 + \frac{dz - \theta}{2d} \left(\frac{t}{\epsilon^z} \right)^2 \right) + \mathcal{O}(t^4). \quad (\text{A.3})$$

Using this result in the canonical momentum from Eq. (4.7) gives

$$P_r = \frac{m(dz - \theta)}{d} \epsilon^{-1-z+\theta/d} t + \mathcal{O}(t^3), \quad (\text{A.4})$$

while the proper momentum from Eq. (4.8) gives

$$P_\rho = \frac{m(dz - \theta)}{d} \epsilon^{-z} t + \mathcal{O}(t^3). \quad (\text{A.5})$$

Thus, at early times, both momenta grow linearly in time, with coefficients proportional to $dz - \theta$. The relativistic AdS limit $z = 1, \theta = 0$ correctly recovers $P_\rho = mt/\epsilon + \mathcal{O}(t^3)$, consistent with Ref. [21].

Turning to late times $r \rightarrow \infty$, the leading behavior of the geodesic follows from the asymptotic form of the velocity, $\dot{r} = r^{1-z}$, which integrates to $r(t) \sim (zt)^{1/z}$. Substituting this into the momentum expressions in Eqs. (4.7) and (4.8) gives the late-time scalings

$$P_r \sim m \epsilon^{\theta/d-z} (zt)^{1-1/z} \quad (\text{A.6})$$

and

$$P_\rho \sim m \epsilon^{\theta/d-z} (zt)^{1-\theta/(dz)}. \quad (\text{A.7})$$

These results match the more rigorous hypergeometric expansion in Eq. (4.14). For $\theta = 0$, they reduce to the Lifshitz scalings $P_r \sim m \epsilon^{-z} (zt)^{1-1/z}$ and $P_\rho \sim m \epsilon^{-z} (zt)^{1-1/z}$, while the AdS limit $z = 1, \theta = 0$ gives the expected $P_r \sim m/\epsilon$ and $P_\rho \sim mt/\epsilon$.

It is also instructive to examine the implications of the null energy condition. In our convention, the physical regime $\theta \leq 0$ implies that the late-time proper momentum scales as $P_\rho \sim t^{1+|\theta|/(dz)}$, which grows faster than linearly. This constitutes a distinctive signature of hyperscaling violation in the holographic Krylov complexity.

Finally, the complexity growth follows directly from $\dot{C}_K = -P_\rho$. The early-time linear growth of the proper momentum integrates to $C_K \sim t^2$, while the late-time scaling $P_\rho \sim t^{1-\theta/(dz)}$ yields $C_K \sim t^{2-\theta/(dz)}$. The Lifshitz limit $\theta = 0$ recovers $C_K \sim t^2$ for all z , and the AdS limit gives the known result $C_K \sim t^2$ with coefficient $m/(2\epsilon)$.

References

- [1] J. M. Maldacena, “The large N limit of superconformal field theories and supergravity,” Adv. Theor. Math. Phys. **2**, 231 (1998) doi:10.4310/ATMP.1998.v2.n2.a1 [hep-th/9711200].

- [2] S. S. Gubser, I. R. Klebanov and A. M. Polyakov, “Gauge theory correlators from non-critical string theory,” *Phys. Lett. B* **428**, 105 (1998) doi:10.1016/S0370-2693(98)00377-3 [hep-th/9802109].
- [3] E. Witten, “Anti-de Sitter space and holography,” *Adv. Theor. Math. Phys.* **2**, 253 (1998) doi:10.4310/ATMP.1998.v2.n2.a2 [hep-th/9802150].
- [4] S. Ryu and T. Takayanagi, “Holographic derivation of entanglement entropy from AdS/CFT,” *Phys. Rev. Lett.* **96**, 181602 (2006) doi:10.1103/PhysRevLett.96.181602 [hep-th/0603001].
- [5] V. E. Hubeny, M. Rangamani and T. Takayanagi, “A covariant holographic entanglement entropy proposal,” *JHEP* **07**, 062 (2007) doi:10.1088/1126-6708/2007/07/062 [arXiv:0705.0016 [hep-th]].
- [6] M. Van Raamsdonk, “Building up spacetime with quantum entanglement,” *Gen. Rel. Grav.* **42**, 2323 (2010) doi:10.1007/s10714-010-1034-0 [arXiv:1005.3035 [hep-th]].
- [7] J. Maldacena, D. Stanford and Z. Yang, “Conformal symmetry and its breaking in two dimensional Nearly Anti-de-Sitter space,” *PTEP* **2016**, 12C104 (2016) doi:10.1093/ptep/ptw124 [arXiv:1606.01857 [hep-th]].
- [8] L. Susskind, “Computational complexity and black hole horizons,” *Fortsch. Phys.* **64**, 24 (2016) doi:10.1002/prop.201500093 [arXiv:1402.5674 [hep-th]].
- [9] L. Susskind, “Entanglement is not enough,” *Fortsch. Phys.* **64**, 49 (2016) doi:10.1002/prop.201500095 [arXiv:1411.0690 [hep-th]].
- [10] A. R. Brown, D. A. Roberts, L. Susskind, B. Swingle and Y. Zhao, “Holographic complexity equals bulk action?,” *Phys. Rev. Lett.* **116**, 191301 (2016) doi:10.1103/PhysRevLett.116.191301 [arXiv:1509.07876 [hep-th]].
- [11] D. E. Parker, X. Cao, A. Avdoshkin, T. Scaffidi and E. Altman, “A universal operator growth hypothesis,” *Phys. Rev. X* **9**, 041017 (2019) doi:10.1103/PhysRevX.9.041017 [arXiv:1812.08657 [cond-mat.stat-mech]].
- [12] E. Rabinovici, A. Sánchez-Garrido, R. Shir and J. Sonner, “Krylov complexity from integrability to chaos,” *JHEP* **07**, 151 (2022) doi:10.1007/JHEP07(2022)151 [arXiv:2207.07701 [hep-th]].
- [13] M. Alishahiha and S. Banerjee, “A universal approach to Krylov state and operator complexities,” *SciPost Phys.* **15**, no.3, 080 (2023) doi:10.21468/SciPostPhys.15.3.080 [arXiv:2212.10583 [hep-th]].
- [14] A. Avdoshkin, A. Dymarsky and M. Smolkin, “Krylov complexity in quantum field theory, and beyond,” *JHEP* **06**, 066 (2024) doi:10.1007/JHEP06(2024)066 [arXiv:2212.14429 [hep-th]].

- [15] H. A. Camargo, V. Jahnke, K. Y. Kim and M. Nishida, “Krylov complexity in free and interacting scalar field theories with bounded power spectrum,” *JHEP* **05**, 226 (2023) doi:10.1007/JHEP05(2023)226 [arXiv:2212.14702 [hep-th]].
- [16] A. Bhattacharyya, S. S. Haque, G. Jafari, J. Murugan and D. Rapotu, “Krylov complexity and spectral form factor for noisy random matrix models,” *JHEP* **10**, 157 (2023) doi:10.1007/JHEP10(2023)157 [arXiv:2307.15495 [hep-th]].
- [17] K. Adhikari, A. Rijal, A. K. Aryal, M. Ghimire, R. Singh and C. Deppe, “Krylov Complexity of Fermionic and Bosonic Gaussian States,” *Fortsch. Phys.* **72**, no.5, 2400014 (2024) doi:10.1002/prop.202400014 [arXiv:2309.10382 [quant-ph]].
- [18] M. Alishahiha and M. J. Vasli, “Thermalization in Krylov basis,” *Eur. Phys. J. C* **85**, no.1, 39 (2025) doi:10.1140/epjc/s10052-025-13757-2 [arXiv:2403.06655 [quant-ph]].
- [19] P. Nandy, A. S. Matsoukas-Roubeas, P. Martínez-Azcona, A. Dymarsky and A. del Campo, “Quantum dynamics in Krylov space: Methods and applications,” *Phys. Rept.* **1125-1128**, no.June 18, 1-82 (2025) doi:10.1016/j.physrep.2025.05.001 [arXiv:2405.09628 [quant-ph]].
- [20] P. Caputa, B. Chen, R. W. McDonald, J. Simón and B. Strittmatter, “Spread complexity rate as proper momentum,” *Phys. Rev. D* **113**, no.4, L041901 (2026) doi:10.1103/7zs8-9zpg [arXiv:2410.23334 [hep-th]].
- [21] Z. Y. Fan, “Momentum-Krylov complexity correspondence,” [arXiv:2411.04492 [hep-th]].
- [22] A. Fatemiabhari, H. Nastase, C. Nunez and D. Roychowdhury, “Holographic Krylov complexity in confining gauge theories,” [arXiv:2511.22717 [hep-th]].
- [23] A. Fatemiabhari and C. Nunez, “Krylov Complexity, Confinement and Universality,” [arXiv:2602.17757 [hep-th]].
- [24] D. Zoakos, “Holographic Krylov complexity in the Coulomb branch of $\mathcal{N} = 4$ SYM,” [arXiv:2603.15435 [hep-th]].
- [25] H. Nastase, C. Nunez and D. Roychowdhury, “Holographic Krylov Complexity for Charged, Composite and Extended Probes,” [arXiv:2604.07432 [hep-th]].
- [26] S. Kachru, X. Liu and M. Mulligan, “Gravity duals of Lifshitz-like fixed points,” *Phys. Rev. D* **78**, 106005 (2008) doi:10.1103/PhysRevD.78.106005 [arXiv:0808.1725 [hep-th]].
- [27] M. Taylor, “Non-relativistic holography and Lifshitz spacetimes,” *Class. Quant. Grav.* **33**, 033001 (2016) doi:10.1088/0264-9381/33/3/033001 [arXiv:1512.03599 [hep-th]].
- [28] E. Kiritsis and J. Ren, “Holographic complexity and hyperscaling violation,” *JHEP* **09**, 089 (2015) doi:10.1007/JHEP09(2015)089 [arXiv:1504.07265 [hep-th]].

- [29] S. A. Hartnoll, A. Lucas and S. Sachdev, “Holographic quantum matter,” arXiv:1612.07324 [hep-th].
- [30] J. Maldacena, S. H. Shenker and D. Stanford, “A bound on chaos,” JHEP **08**, 106 (2016) doi:10.1007/JHEP08(2016)106 [arXiv:1503.01409 [hep-th]].
- [31] N. Ogawa, T. Takayanagi, and T. Ugajin, “Holographic Fermi surfaces and entanglement entropy,” JHEP **01** (2012) 125 [arXiv:1111.1023].
- [32] M. R. Mohammadi Mozaffar and A. Mollabashi, “Entanglement in Lifshitz-type Quantum Field Theories,” JHEP **07**, 120 (2017) doi:10.1007/JHEP07(2017)120 [arXiv:1705.00483 [hep-th]].
- [33] T. He, J. M. Magan and S. Vandoren, “Entanglement Entropy in Lifshitz Theories,” SciPost Phys. **3**, no.5, 034 (2017) doi:10.21468/SciPostPhys.3.5.034 [arXiv:1705.01147 [hep-th]].
- [34] S. A. Gentle and S. Vandoren, “Lifshitz entanglement entropy from holographic cMERA,” JHEP **07**, 013 (2018) doi:10.1007/JHEP07(2018)013 [arXiv:1711.11509 [hep-th]].
- [35] M. R. Mohammadi Mozaffar and A. Mollabashi, “Logarithmic Negativity in Lifshitz Harmonic Models,” J. Stat. Mech. **1805**, no.5, 053113 (2018) doi:10.1088/1742-5468/aac135 [arXiv:1712.03731 [hep-th]].
- [36] M. R. Mohammadi Mozaffar and A. Mollabashi, “Entanglement Evolution in Lifshitz-type Scalar Theories,” JHEP **01**, 137 (2019) doi:10.1007/JHEP01(2019)137 [arXiv:1811.11470 [hep-th]].
- [37] M. R. Mohammadi Mozaffar and A. Mollabashi, “Universal Scaling in Fast Quenches Near Lifshitz-Like Fixed Points,” Phys. Lett. B **797**, 134906 (2019) doi:10.1016/j.physletb.2019.134906 [arXiv:1906.07017 [hep-th]].
- [38] D. Hartmann, K. Kavanagh and S. Vandoren, “Entanglement entropy with Lifshitz fermions,” SciPost Phys. **11**, no.2, 031 (2021) doi:10.21468/SciPostPhys.11.2.031 [arXiv:2104.10913 [quant-ph]].
- [39] M. Mintchev, D. Pontello, A. Sartori and E. Tonni, “Entanglement entropies of an interval in the free Schrödinger field theory at finite density,” JHEP **07**, 120 (2022) doi:10.1007/JHEP07(2022)120 [arXiv:2201.04522 [hep-th]].
- [40] M. R. M. Mozaffar and A. Mollabashi, “Time scaling of entanglement in integrable scale-invariant theories,” Phys. Rev. Res. **4**, no.2, L022010 (2022) doi:10.1103/PhysRevResearch.4.L022010 [arXiv:2106.14700 [hep-th]].
- [41] M. Mintchev, D. Pontello and E. Tonni, “Entanglement entropies of an interval in the free Schrödinger field theory on the half line,” JHEP **09**, 090 (2022) doi:10.1007/JHEP09(2022)090 [arXiv:2206.06187 [hep-th]].

- [42] M. J. Vasli, K. Babaei Velni, M. R. Mohammadi Mozaffar, A. Mollabashi and M. Alishahiha, “Krylov complexity in Lifshitz-type scalar field theories,” *Eur. Phys. J. C* **84**, no.3, 235 (2024) doi:10.1140/epjc/s10052-024-12609-9 [arXiv:2307.08307 [hep-th]].
- [43] H. R. Imani, K. Babaei Velni and M. R. Mohammadi Mozaffar, “Krylov complexity in Lifshitz-type Dirac field theories,” *Eur. Phys. J. C* **85**, no.9, 958 (2025) doi:10.1140/epjc/s10052-025-14669-x [arXiv:2506.08765 [hep-th]].
- [44] M. R. Mohammadi Mozaffar and A. Mollabashi, “Symmetry resolved entanglement in Lifshitz field theories,” [arXiv:2604.19082 [hep-th]].
- [45] A. Fatemiabhari, C. Nunez and R. T. Santamaria, “Complexity and Operator Growth in Holographic 6d SCFTs,” [arXiv:2603.10106 [hep-th]].
- [46] A. Donos and J. P. Gauntlett, “Lifshitz Solutions of D=10 and D=11 supergravity,” *JHEP* **12** (2010), 002 doi:10.1007/JHEP12(2010)002 [arXiv:1008.2062 [hep-th]].
- [47] X. Dong, S. Harrison, S. Kachru, G. Torroba and H. Wang, “Aspects of holography for theories with hyperscaling violation,” *JHEP* **1206**, 041 (2012) doi:10.1007/JHEP06(2012)041 [arXiv:1201.1905 [hep-th]].
- [48] M. Alishahiha, E. O. Colgain and H. Yavartanoo, “Charged Black Branes with Hyperscaling Violating Factor,” *JHEP* **1211**, 137 (2012) doi:10.1007/JHEP11(2012)137 [arXiv:1209.3946 [hep-th]].
- [49] K. Bitaghsir Fadafan and F. Saiedi, *Eur. Phys. J. C* **75** (2015) no.12, 612 doi:10.1140/epjc/s10052-015-3839-1 [arXiv:1504.02432 [hep-th]].
- [50] J. Gath, J. Hartong, R. Monteiro and N. A. Obers, “Holographic Models for Theories with Hyperscaling Violation,” *JHEP* **1304**, 159 (2013) doi:10.1007/JHEP04(2013)159 [arXiv:1212.3263 [hep-th]].
- [51] M. Alishahiha, A. Faraji Astaneh and M. R. Mohammadi Mozaffar, “Thermalization in backgrounds with hyperscaling violating factor,” *Phys. Rev. D* **90**, no. 4, 046004 (2014) doi:10.1103/PhysRevD.90.046004 [arXiv:1401.2807 [hep-th]].
- [52] M. Alishahiha, A. Faraji Astaneh, M. R. Mohammadi Mozaffar and A. Mollabashi, “Complexity Growth with Lifshitz Scaling and Hyprscaling Violation,” *JHEP* **1807**, 042 (2018) doi:10.1007/JHEP07(2018)042 [arXiv:1802.06740 [hep-th]].
- [53] G. T. Horowitz and B. Way, “Lifshitz Singularities,” *Phys. Rev. D* **85**, 046008 (2012) [arXiv:1111.1243].
- [54] S. A. Gentle and C. Keeler, “On the reconstruction of Lifshitz spacetimes,” *JHEP* **03**, 195 (2016) [arXiv:1512.04538].

- [55] K. Copsey and R. B. Mann, “Hidden singularities and closed timelike curves in a proposed dual for Lifshitz-Chern-Simons gauge theories,” *JHEP* **03**, 039 (2011) [arXiv:1112.0578].